Effects of solvents on Li+ distribution and dynamics in PVDF/LiFSI solid polymer electrolytes: An all-atom molecular dynamics simulation study

Mohammed Lemaalem, Philippe Carbonnière

Version of Record: https://www.sciencedirect.com/science/article/pii/S0167273823001625
Manuscript_4ef23b7ab4fd8014f7281236d7cd0eda

Effects of solvents on Li^+ distribution and dynamics in PVDF/LiFSI solid polymer electrolytes: An all-atom Molecular Dynamics simulation study.*

Mohammed Lemaalem,[a,*], and Philippe Carbonniere,[a,*]

[a] *Université de Pau et des Pays de l'Adour, E2S UPPA, CNRS, IPREM UMR5254, Institut des Sciences Analytiques et de Physico-chimie pour l'Environnement et les Matériaux, Helioparc, Pau, France.*

Abstract

Large-scale all-atom molecular dynamics simulations are employed to investigate the structure and dynamics of solid polymer electrolytes (SPEs) models composed of polyvinylidene fluoride (PVDF) as the polymer matrix, lithium bis(fluorosulfonyl)imide salt (LiFSI), and six different types of solvents in varying proportions. The influence of solvents on the physicochemical parameters of SPEs relevant to the Li-ion battery sector is analyzed. We demonstrate that solvents containing oxygen atoms exhibit varying abilities to dissociate LiFSI ions, form confined channels in the SPEs, and reduce PVDF crystallinity. Moreover, certain solvents with a strong affinity for cations promote the assembly of Li^+ transport into nano-domains separate from the PVDF chains, resulting in a significant reduction in the Li^+ transference number (t_{Li^+}) when present in high concentrations. Conversely, ionic conductivity is enhanced while maintaining a good t_{Li^+} for solvents with high mobility that form small clusters of Li^+-solvent complexes. Our nanoscale investigations provide insights into approaches for improving ionic conductivity and controlling ion arrangement in SPEs, which are crucial for optimal battery performance, achieved by selecting a suitable solvent with a regulated quantity.

Keywords: `PVDF/LiFSI Solid Polymer Electrolyte, Molecular dynamics simulations, Solvent effect, Ionic conductivity.`

*Corresponding author: mohammed.lemaalem@univ-pau.fr; philippe.carbonniere@univ-pau.fr

*Supplementary electronic information is available.

1. Introduction

Solid polymer electrolytes (SPEs) hold great promise as a viable solution for the cutting-edge All-Solid-State Li-Batteries (AllSSLiB), offering a sustainable energy production alternative and reducing long-term reliance on fossil fuels [1]. The SPEs demonstrate high thermal stability, mechanical strength, device simplicity, and energy density [2][3]. However, the overall performance of these electrolytes is limited by their crystallinity and low ionic conductivity under typical operating conditions, limiting their massive commercial implementation [4][5]. Thus, there is a high demand for developing new concepts and materials to enhance the conductivity of the SPEs, at room temperature.
Despite the broad range of potential ways to improve the performance of existing SPEs, it has been noted that ion transport occurs mainly in the amorphous region of the electrolyte, which is characterized by a high polarity and can promote a higher salt dissociation [3][5]. Experimental studies demonstrate that adding molecular solvents [6][7][8][9][10][11] with a high dielectric constant or ionic liquids as a plasticizer promotes higher ionic conductivities [12][13][14][15][16][17][18][19][20]. Nevertheless, the solvents increase the overall amorphous fraction, reduce the polymer crystallinity, and yield a loss of mechanical strength of the SPEs [17]. Besides, they increase the overall polarity and affect the polymer chains/salts interaction [21][22].

In this paper, our focus is on investigating the impact of various solvents present in small quantities in PVDF/LiFSI solid polymer electrolytes (SPEs). These solvents can either be residues from the SPEs preparation process or intentionally added during battery assembly. When used as a binder in electrode formulation and separator design, PVDF/LiFSI SPEs offer numerous advantages for the lithium battery industry. When a small amount of solvent is added to the polymer matrix, the resulting SPEs typically form thin and flexible films. Unlike gel polymer electrolytes, which involve a solid polymer matrix swollen with a liquid electrolyte, SPEs maintain their solid-state nature. PVDF exhibits favorable electrochemical and mechanical stability, making it a commonly used polymer in commercial lithium-ion batteries. Unlike polyethylene oxide (PEO), PVDF has limited intermolecular interactions with lithium ions (Li^+) [23][24], thereby minimizing the degradation of composite structures during repeated charge and discharge cycles. Thus, PVDF exhibits limited reactivity towards Li^+ diffusion. Previous studies on solvent-containing PEO polymer electrolytes have shown that higher solvent content typically leads to cation solvation, resulting in increased cation mobility, higher ionic conductivity, and altered polymer structure [25][26]. Solvents have a plasticizing effect on commonly used polymers like PEO, resulting in lower Tg values for amorphous polymer fractions, reduced crystallinity, and enhanced side-chain mobility [27][28][29][30]. Notably, the amount of adsorbed solvent significantly impacts solid polymer electrolytes [31]. DMF, NMP, and DMSO are frequently employed solvents for preparing PVDF/LiFSI electrolytes [32]. Zhou et al. investigated the effects of these solvents on ionic conductivity in PDVF-LiTFSI electrolytes [27]. They

found that DMF enhances conductivity by facilitating Li^+ motion, but its removal from polymer electrolytes is challenging due to its high boiling point [33]. Łatoszyńska et al. studied the impact of DMF and NMP on ionic conductivity in PVDF/LiFSI SPEs [34]. They observed that DMF has a greater influence compared to NMP. FEC, DME, and ES are used as additives to enhance the electrode/electrolyte interface in batteries [35][36][37].

Notwithstanding the substantial impact of solvents on cutting-edge battery performance, their presence in the SPEs is often underreported. While extensive research has focused on the interaction between solvents and lithium metal [38][39][40][41], there is a lack of information regarding the effects of solvents in SPEs, notably for PVDF/LiFSI SPEs, and their implications for battery performance. Consequently, there is a pressing need to employ nanoscale resolution techniques, such as molecular dynamics (MD), to heighten our comprehension of these systems [42][43][44][45][46][47]. Investigating the influence of solvents at the atomistic level in PVDF/LiFSI SPEs enables rational selection of solvent type and quantity for SPEs preparation, facilitating dendrite suppression near the anode and enhanced ionic conductivity. This study aims to elucidate the impact of solvents on the diffusion behavior of LiFSI ions within PVDF/LiFSI SPEs. We consider six solvents: Ethylene Sulfite (ES), Dimethyl Ether (DME), Fluoroethylene Carbonate (FEC), Dimethylformamide (DMF), N-Methyl-2-pyrrolidone (NMP), and Dimethylsulfoxide (DMSO), varying their concentrations. Specifically, we investigate the solvent's effect on PVDF chain conformation and dynamics, as well as the Li^+-FSI^- and Li^+-solvent interactions, Li^+ coordination number, and the formation of ion-ion and Li^+-solvent clusters. Our systematic analysis compares these findings with those obtained for pure PVDF and solvent-free PVDF+LiFSI systems, elucidating the structure-dynamics relationships governing solvent effects in PVDF/LiFSI SPEs.

2. Material and methods

The SPEs model consisted of a mixture of 12 PVDF chains containing 150 carbons per chain, 20% polymer molecular weight lithium bis(fluorosulfonyl)imide (LiFSI) salt, i.e., 30 carbons/LiFSI giving 60 LiFSIs, and different types and amounts of solvents. The solvent content relative to the LiFSI ions content is quantified using molar fractions, denoted as n(solvent)/n(LiFSI), with values of 0 (no solvent), 0.3 (18 solvent molecules), 0.6 (36 solvent molecules), 1 (60 solvent molecules), 2 (120 solvent molecules), and 3 (180 solvent molecules). Figures 1a and 1b illustrate the compositions of the simulated systems for the case of $n(solvent)/n(Li^+) = 3$. The OPLS-AA force field was used for the PVDF chains and solvent molecules interaction potential models [48][49], while the CL&P force field was used for the ions [50]. Both force field models use Lennard-Jones and Coulombic potentials to capture non-bonded interactions. The geometric mixing rule is applied to combine the interaction parameters between different atom pairs, ensuring an accurate representation of the system's interactions

[51]. Molecular dynamics (MD) simulations were performed using the LAMMPS software package [51], applying three-dimensional periodic boundary conditions and a cutoff distance of 12Å for Lennard-Jones and Coulomb interactions. A time-step of δt = 1 fs was used for all simulated cases [51].

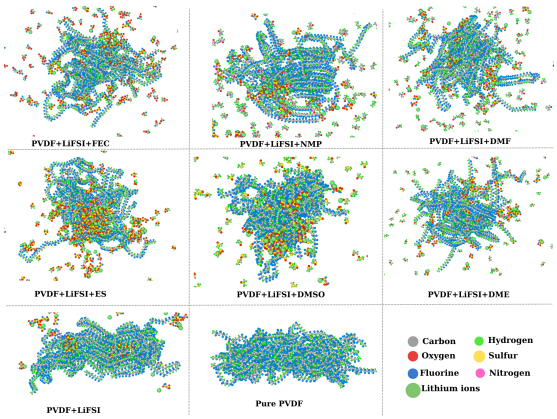

(a)

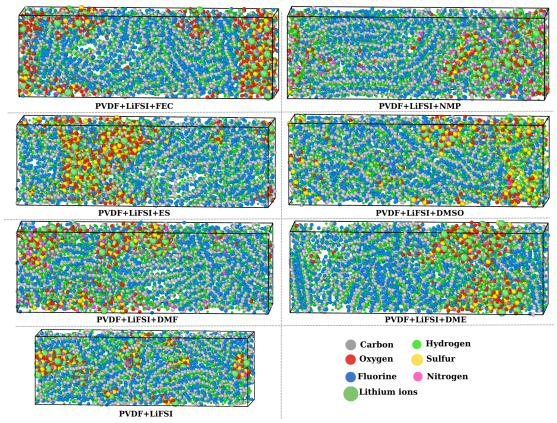

(b)

Figure 1: Captions of simulated SPEs systems, pure PVDF chains, 12PVDF+20%LiFSI, and 12PVDF+20%LiFSI+solvent (n(solvent)/n(Li^+)=3). (a), the periodic boundary conditions (PBC) are unwrapped to visualize the conformation of the PVDF chains. (b), The PBC are wrapped to visualize the ionic liquid distribution.

The initial configuration, generated using the Moltemplate package [52], consists of parallel-packed polymer chains, separated by 10 Å, and randomly dispersed solvents and salts molecules, within the PVDF chains, into an oversized orthorhombic box. The chains consist of 100% β-phase PVDF, indicating that

Table 1: Equilibrated box lengths of the simulated SPEs systems for different solvent types and amounts (n denotes n(solvent)/n(LiFSI)).

	Simulation box lengths (Å)					
solvent	DMF	FEC	NMP	DME	ES	DMSO
n	Lx; Ly=Lz	Lx; Ly=Lz	Lx; Ly=Lz	Lx; Ly=Lz	Lx; Ly=Lz	Lx; Ly=Lz
0.3	93.3; 29.9	93.5; 29.9	93.9; 30.0	91.3; 29.2	91.8; 29.4	91.1; 29.2
0.6	93.7; 29.9	93.6; 29.9	93.9; 30.0	93.5; 29.9	93.5; 29.9	92.2; 29.5
1	94.8; 30.4	95.5; 30.6	95.9; 30.7	94.0; 30.0	95.5; 30.6	92.9; 29.8
2	97.1; 31.1	96.8; 31.0	97.9; 31.4	94.6; 30.3	96.0; 30.7	95.0; 30.4
3	100.0; 32.0	100.3; 32.1	102.1; 32.7	98.0; 31.4	101.1; 32.4	97.7; 31.3

they are initially in the form of straight linear structures. Before running the MD simulation production stage, the initial structures are sufficiently equilibred in order to adjust the simulation box volume. In the equilibration process, the energy of each simulated system was minimized to correct the bond lengths, ensure the optimal particle distribution, and thus avoid divergence in the thermodynamics equilibrium. The energy minimization algorithm consists of adjusting particle coordinates iteratively [51]. A finite unitless stopping tolerance for energy (Estop=10^{-7}) that represents the energy variation between consecutive iterations divided by the energy magnitude, and a stopping tolerance for force (Fstop=10^{-8} kcal Å^{-1}) are chosen. The equilibrium corresponds to the minimum energy acquired at t$\sim$ 0.1 ns for all simulated cases. After that, the system is agitated using the Langevin thermostat at T=900 K for another t=1 ns, followed by the same process using the Nosé–Hoover thermostat [51]. Then, to reach the desired ambient condition of temperature and pressure (T=300 K, P=1 bar), the simulated systems were equilibrated in the NPT-statistical ensemble using the Berendsen barostat [51]. Firstly, from T=900K to T=303 K at constant pressure P=500 bar, to force the systems to reach the convenable temperature for t=1 ns. Secondly, the pressure is decreased from P=500 bar to P=1 bar at constant temperature T=303 K, to attain the convenable volume for t=1 ns. In the last performed NPT equilibration stage, the systems were equilibrated at room temperature and ambient pressure (T=303 K, P=1 bar) for t=10 ns, forcing them to achieve the experimental densities. Finally, we run the simulations for a long time up to t=190 ns to produce the static and dynamic properties in the NVT-statistical ensemble using the Nosé–Hoover thermostat at T=303 K and fixed volume. We calculated the evolution of the main static and dynamics properties in these systems, i.e., the self-diffusion coefficients of each component from the mean-square-displacements, the ionic conductivity, and Li^+ transference number, the ions distribution, the mean distances between the ions and the solvent and between the Li^+ and FSI^-, the Li^+ coordination number, and the size of formed clusters. Additional computational details and complementary results are provided in the Supporting Information. The PVDF chains are simulated separately (without introducing the LiFSI and solvent) to

test the efficiency of the NPT equilibration process (see Figure S1). From the analyses of the NPT simulation, the simulation box volume variation remains practically steady after three ns of the final equilibration stage. The volume at the last seven ns is 5,53 $10^{-26} \pm 0.1$ Å^3, which gives a mass density of 1.73 $\pm$ 0.3 g/cm^{-3}. The obtained value covers the PVDF experimental density value 1.7 g/cm^{-3} [53]. The equilibrated boxes size of the simulated SPEs systems are summarized in Table 1. We note that during the volume equilibration, the only condition imposed is that the direction perpendicular to the chain's length varies equally. As a result, the optimized volume is found to be orthorhombic. However, to investigate the initial polymer setup on the structure of the chains, we conducted another simulation by starting with randomly oriented chains into an oversized cubic box and imposing equal variation in all box directions. In this case, the equilibrated volume is cubic. Interestingly, a comparison of the polymer structures from the radial distribution function curves depicted in Figure S1 in the two volumes' shapes showed no significant differences. Besides, it is noted that the simulation box shape, whether orthorhombic or cubic, does not affect the SPEs properties significantly because periodic boundary conditions are applied, ensuring the proper interaction between particles across the boundaries, and because after conducting a long-duration MD simulation lasting up to 200 ns, the distribution of particles within the solid polymer electrolyte undergoes rearrangement of positions and velocities each time step (1 fs), which is only contingent upon the type of the used solvent.

3. Results

Figure 2a presents the calculated values of ionic conductivity at room temperature and ambient pressure (T=300 K, P=1 bar) for solid polymer electrolytes (SPEs) containing varying amounts of confined solvents, systematically compared to solvent-free PVDF+20% molecular weight LiFSI. According to Figure 2a, the ionic conductivity increases by increasing the NMP, FEC, and DMF solvent amounts and decreases by increasing the ES and DMSO amounts. For DME, a significant increase is observed until n(solvent)/n(Li^+)=1. Then, the ionic conductivity drastically decreases with increasing the solvent amount. The variation in the ionic conductivity is mainly due to a decrease in the Li^+ diffusion related to the solvation effect and the size of formed clusters. These properties are discussed in detail in section 3.3. Thus, DMF, FEC, NMP, and DME can be considered excellent for ionic conductivity improvement. Figure 2b depicts the Li^+ transference number versus solvent type and amount. Accordingly, the transference number decreases rapidly with ES, DME and DMSO solvent presence and moderatly with NMP, DMF, and FEC. The reason for the rapid decay, especially for ES and DME solvents, is that the movement of Li^+ ions is sensitive to small amounts of solvent. As the amount of solvent increases, the coordination shell around the Li^+ ion is significantly increased for ES and DME solvents and moderately for the other solvents. The significant increase in the number of solvent around the Li^+ ions results in a significant decrease in the Li^+ dynamics and then in the Li^+ transference number. The dependence of

the Li^+ diffusion on the coordination environnement will be discussed in detail in sections 3.2 and 3.3.

Figures S2 and S3 depict examples of the log-log plot of the MSD as a function of time, showing the normal diffusion regime for Li^+ and FSI^-, calculated from our MD simulations. In Figure S4a, we present the normal diffusion-coefficient (D_{Li^+}) for the Li^+ cations as a function of the solvent amounts for all considered solvents. We recall that the ionic conductivity depends on the number density of ions, the temperature, and the diffusion of the ions impacted by the time duration at which ions are caged by the surrounding particles (See Figures S4a and S4b). Here, we fixed the temperature and the number of ions. However, some slight volume variations are observed during the equilibration phases, due to the nature of the solvent. Therefore, the variation of σ results from the variation diffusion of ions (cf. Figure S4a and Figure 2a).
To elucidate the underlying significance of the solvent in the PVDF/LiFSI SPEs, we rigorously analyze the structural properties to ascertain the intricate interplay between the structural characteristics and dynamic behavior of the (Li^+, FSI^-) ions.

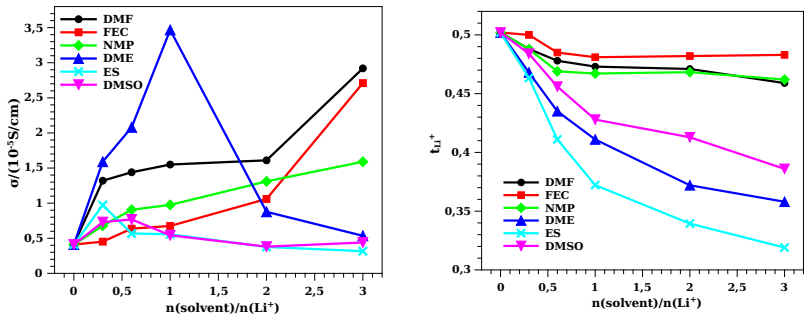

(a) (b)

Figure 2: (a) Ionic conductivity values (σ) as a function of solvents/ions molar fraction. (b) Li^+ transference number (t_{Li^+}) as a function of solvents/ions molar fraction.

3.1. Effect of solvent on the PVDF chains conformation

The addition of solvents has been shown to enhance the lithium salt ions' mobility by decreasing their affinity to polymers that have an attractive interaction with the ions [54][55][56][57]. In the case of PVDF/LiFSI SPEs, the electrostatic attraction of Li^+ by the Fluor from PVDF is weak (Figure S5) compared to that from the Oxygens atoms from solvents and FSI^- (Figure 5a). Thus, the solvents increase the ionic conductivity by dissociating the ions and thus increasing their diffusion, playing the role of transporter, as detailed in the following sections. FEC interact with the PVDF chains more than the other considered solvent, as

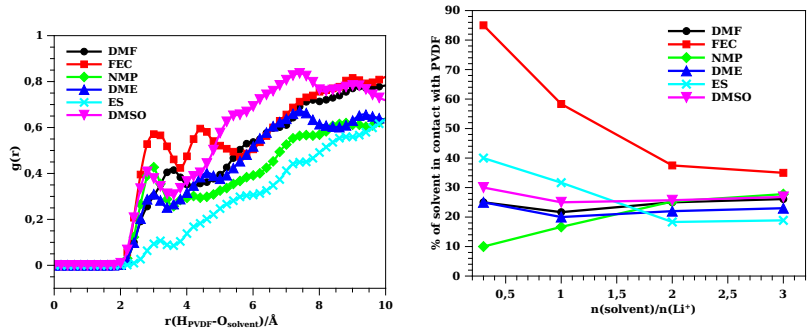

(a)

(b)

(c)

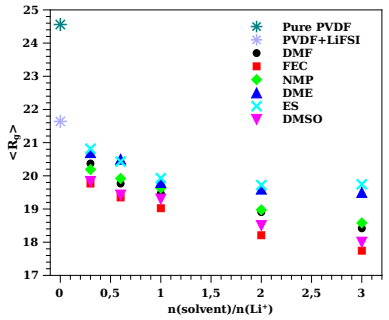

(d)

(e)

Figure 3: **(a)** Radial distribution functions g(r) of O(solvents)–H(PVDF) for n(solvent)/n(Li^+)=3, **(b)** % of solvents in contact with PVDF chains within a distance of 4 Å, **(c)** the mean value of the radius of gyration over the 12 PVDF chains, R_g.

depicted in Figures 3a and 3b. Then, FEC create ripples in the contact surface with the polymer chains making them more amorphous, and thus the chain dynamics increased, as depicted in Figure S6a. For pure PVDF, the polymer chains extend into a predominantly linear conformation (cf. Figure 1a). When ions and solvents are added, the repulsion between monomers decreases, and the PVDF chains tend to adopt a globular conformation. This tendency can be seen qualitatively in Figure 1 and quantitatively in Figure 3a. Our MD simulation results suggest that the PVDF chains have a lower affinity for ES, DME, DMF, NMP, and DMSO than FEC (Figure 3b). We note that the obtained radius of gyration is compared to the Flory Scaling-Law: $R_g = aN^{\mu}$, with a a scaling factor ($a \approx 2$), N the polymerization degree (N=75), and μ a critical

exponent, $\mu \approx 1/2$ for the conformation of the globular chain and $\mu \approx 3/5$ for the conformation of the extended chain.

3.2. Effect of solvent on the Li^+ ions clustering

Figure 4a shows the percentage of dissociated ions. Here, we mean the ions found to have a separation distance of more than 4 Å for all ions combinations, Li^+-Li^+, FSI^--FSI^-, and Li^+-FSI^-. Figure 4b shows the mean values of the Li^+-FSI^- aggregates with a separation distance of 4 Å or less defined as Li^+-FSI^- clusters. The size of Li^+-FSI^- clusters is calculated by the number of Li^+ and Nitrogen atom, as it is the center of FSI^-, connected between them. Statistical details of the Li^+-Li^+ and FSI^--FSI^- clusters are presented and commented on in Figure S7.

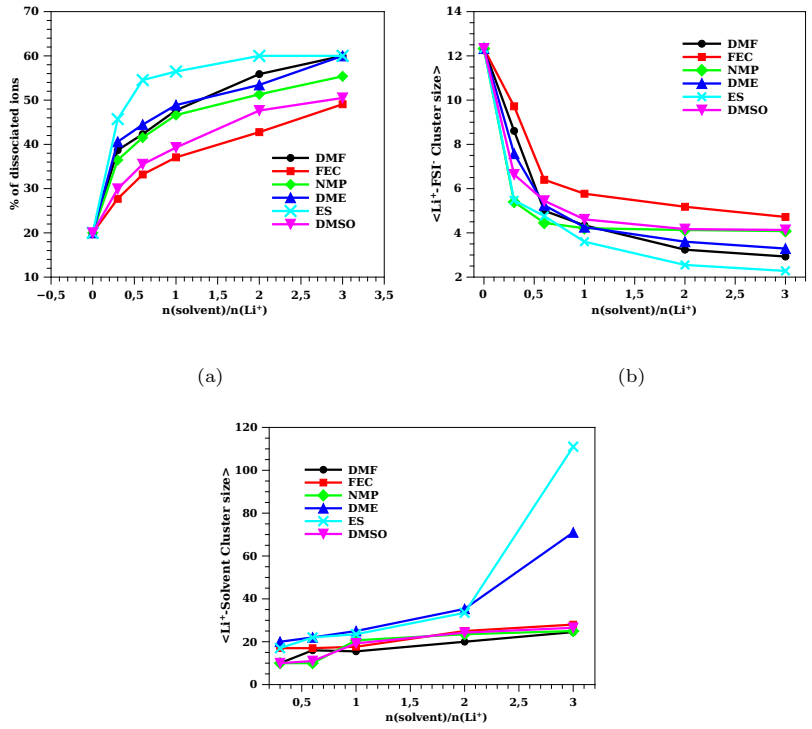

(a) (b)

(c)

Figure 4: **(a)** the % of dissociated ions,**(b)** and **(c)** depict the mean sizes of formed clusters of Li^+-FSI^- and Li^+-solvent, respectively, as a function of solvent types and amounts.

We note that the size of Li^+-FSI^- cluster formed in the PVDF/LiFSI SPEs decreases with increasing the solvent amount for all considered solvents. However, different solvents appear to cause diverse arrangements of the Li^+-FSI^-

ions and PVDF microstructures. As discussed in the previous section, the PVDF chains are solvated by the FEC, DMF, and NMP. Besides, the ions are dispersed in the volume. The higher affinity of FEC, DMSO, and NMP to the PVDF than the cations decreases the Li^+ solvation (Figure 4a). Thus, the Li^+-FSI^- clusters formed in the PVDF/LiFSI SPEs with the presence of these solvents are bigger (Figure 4b). ES and DME show a low affinity to the polymer chains. They are gathered in separated phases from the PVDF chains and efficiently solvate the ions. Thus, the ions clusters size is decreased. The DMF can solvate both ions and PVDF. Thus, only small Li^+-FSI^- clusters are formed when DMF is introduced with a high amount.

Figure 4c depicts the Li^+-solvent formed clusters analyses. For reference, the average value of the cluster size is performed only over clusters containing ten components or larger. ES and DME are found to form large clusters along with the cations, consequently limiting their diffusion and lowering the transference number drastically (Figure 2b). The other solvents, DMF, FEC, NMP, and DMSO, does not form large clusters along with the Li^+. These findings explain why DMF, FEC, and NMP increase ionic conductivity but not why DMSO does not. Investigations about the diffusion of the solvent (see Figure S6b) show that the DMSO diffuses slowly in PVDF/LiFSI SPEs. So, DMSO makes the SPEs more viscous. Thus, decreasing the Li^+ diffusion. The marginal decrease in the dynamics of DMSO and ES as the solvent content increases in the PVDF/LiFSI solid polymer electrolyte (SPE) can be attributed, in part, to their interaction with the constituents of the SPE, which can affect the dynamics of all components of the SPE. The ES strongly interacts with the cations (see Figure 5a) and forms large aggregates (see Figure 4c). In addition to its relatively high viscosity, i.e., slow dynamic, the DMSO strongly interact with the PVDF chains (see Figure 3a).

3.3. Effect of solvents on the structure around the Li^+

In Figure 5a and 5b, we report the partial Radial-Distribution-Function g(r) versus the separation distance for the pair-wise Li^+-O(FSI^-) and Li^+-O(solvents), respectively, for the highest solvents amounts considered in this work, n(solvent)/n(Li^+)=3. We remark that the Li^+ and Oxygens from solvents and FSI^- show a local order for a separation distance of 1.9 Å$< r <$ 2.4 Å. This local order is due to a strong correlation between Li^+ and the negatively charged Oxygens atoms. Moreover, we note a remarkable shift of the RDF first peak toward the right for ES and DME (Figure 5a). This shift is due to a net dominance of the interaction solvent/Li^+, as depicted in Figure 5b.

Figure 5c depicts the Li^+-FSI^- and Li^+-solvent separation distance for various solvents derived from the Li^+-O interactions. We mention that small distances are equivalent to a high attractive attraction. The r(Li^+-FSI^-) distance rises with increasing solvent quantity for all examined solvents. Moreover, except for FEC, r(Li^+-FSI^-) $>$ r(Li^+-solvent). Furthermore, in the absence of a solvent, the Li^+ ions are trapped by the FSI^- oxygens (Figure 6). When solvent is added, the FSI^- oxygens compete with the solvent oxygens to attract the Li^+ cations (Figure 5c). We assert that the ability of the solvent to dissociate LiFSI

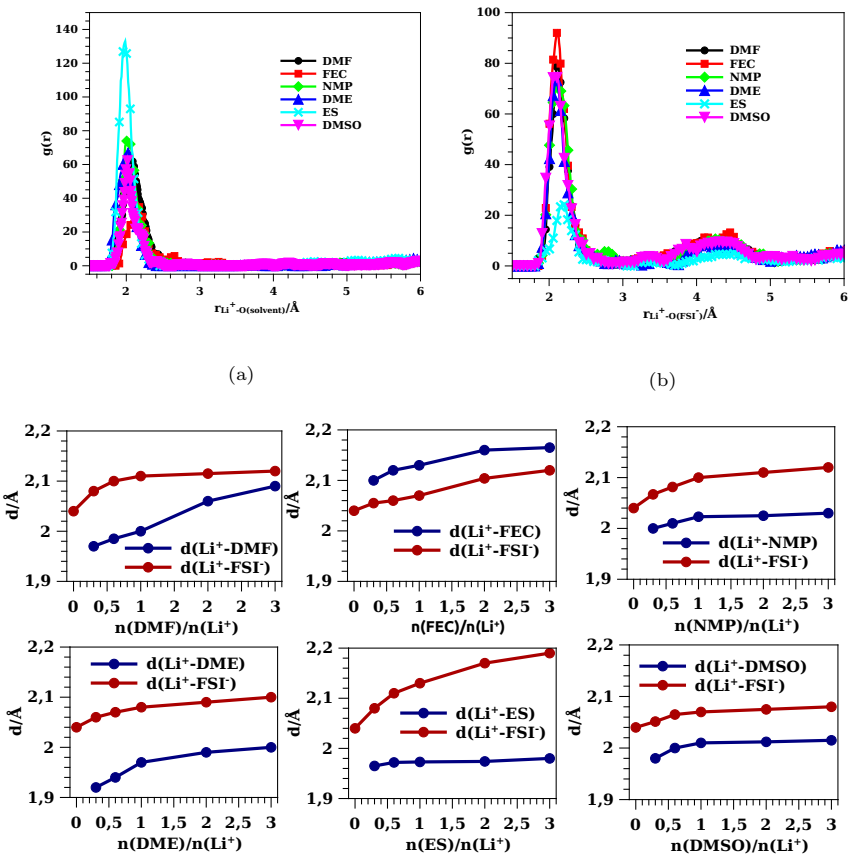

(a) (b)

(c)

Figure 5: Radial distribution functions, g(r), for n(solvent)/n(Li^+)=3, **(a)** g(r) of Li^+-O(solvents), **(b)** g(r) Li^+-O(FSI^-). **(c)** the most probable distances Li^+-FSI^- and Li^+-Solvent, correspond to the computed radial distribution function maximum.

ions can be summarized as follows: ES > DME ≥ DMF > NMP > DMSO ≥ FEC.

The optimal enhancement of ionic conductivity depends on but is not limited to the solvation effect for all considered solvents. By solvating ions, solvents can increase ionic bonding. Moreover, as shown in Figures 2 and 3c and in agreement with experimental results [27][58], they can cause PVDF to be more amorphous. Thus, the ions are freer to move if the solvents do not confine them.

Figure S8 provides the relative statistics of Li^+ coordination by FSI^- and solvents in the SPEs studied system. Although the cations are predominantly

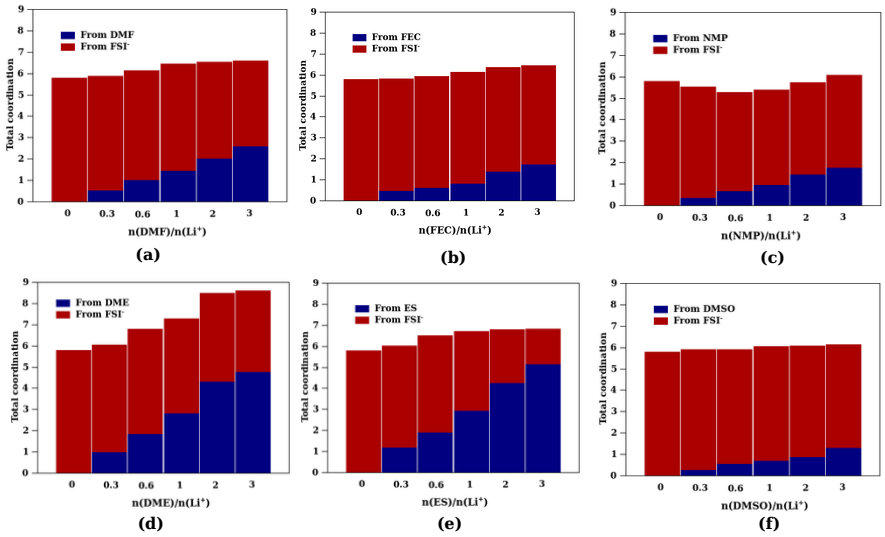

Figure 6: The mean values of the total coordination of Li^+ by negatively charged atoms from FSI^- and solvent molecules for different solvent types and amounts, as calculated from the statistical distributions depicted in Figure S8.

coordinated by the Oxygens atoms from solvents and anions, we consider all negatively charged particles from either the FSI^- anions or the solvent molecules or both for calculating the total coordination surrounding each cation within a sphere of radius 3.5 Å. This distance is sufficient to consider the Nitrogen and Fluor coordination from the FSI^- and other negatively charged particles than Oxygens from solvents, and also the fluctuations resulting from the thermal agitation. Figure 6 presents the mean coordination values and their relationship to the solvent type and content. We note the Li^+ coordination number from solvents increases as the solvent quantity increases, but the Li^+ coordination from FSI^- decreases. These statements are connected to solvents' capacity to dissociate ions (Figure. 5c). The solvents play a substantial role in the coordination of Li^+ notably when they exist with a significant amount (n(solvent)/n(Li^+)>1). In particular, for ES and DME, the Li^+ coordination from the solvents is greater than the FSI^- anions. The Li^+ total coordination number is slightly modified around 6 for different solvent types and amounts, except we note that the total coordination number from the DME is increased proportionally to the DME amount within a range of 6-9. This high coordination number can be related to the fact that DME has a great affinity to the Li^+ and also to the fact that DME is a small molecule. Hence, it can be concluded that DME molecules have a higher propensity to coordinate with Li^+ ions, surpassing other solvents in terms of their Li^+ coordination capacity.

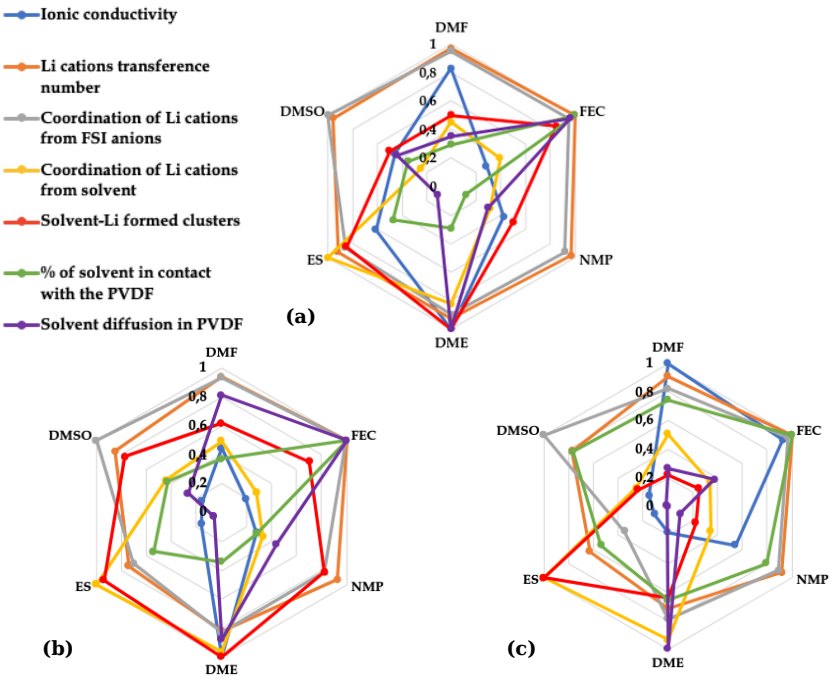

Figure 7: Radar plots comparing pertinent calculated properties related to the solvent type and amount. **(a)** n(solvent)/n(Li^+)=0.3, **(b)** n(solvent)/n(Li^+)=1, **(c)** n(solvent)/n(Li^+)=3. To facilitate the comparison, the values corresponding to each effect, presented throughout the paper, are each time normalized by the maximum value.

4. Discussion

DMF, NMP, and DMSO are typical solvents to prepare the PVDF electrolyte through solvent casting [32]. In this context, Zhou et al. prepared a series of PDVF-LiTFSI electrolytes with DMF, NMP, DMSO, and dimethylacetamide (DMA) to quantify the effects of these trapped solvents, encompassing NMP, DMF, and DMSO, on the ionic conductivity [27]. They found an ionic conductivity around 10^{-5} S/cm depending on the solvent type and amount, comparable with our MD simulation results, presented in Figure 2a. According to this experimental study, DMF is absorbed inside the PVDF and increases the ionic conductivity by facilitating the Li^+ motion. Besides, regarding its high boiling point (150 °C), DMF is complicated to remove from polymer electrolytes despite applicating substantial drying procedures [33]. In another similar work, Łatoszyńska et al. investigated the effect of DMF and NMP on the ionic conductivity in PVDF/LiFSI SPEs [34]. They found that DMF has a more significant impact on ionic conductivity in the electrolyte than NMP. In line with our all-atom MD simulation results, the slight influence of NMP and DMSO on increasing the ionic conductivity compared to DMF was attributed

to their slow dynamics in the PVDF matrix (Figure S6b), i.e., higher viscosity. Furthermore, for DMF, the interaction Li^+-PVDF is noteworthy compared to NMP and DMSO, as can be witnessed from the g(r) Li^+-F(PVDF) curves depicted in Figure S5. Consequently, as discussed in Ref. [30], the mobility of the Li^+ cations is increased with the presence of solvents that attract the cations more than the polymer chains noting that the opposite is true (Figure S4a). Accordingly, the ionic conductivity in the presence of DMSO is lesser compared to DMF and NMP (Figure 2a).

FEC, DME, and ES are used in the PVDF/LiFSI SPEs as additives to enhance the Lithium-Ion Batteries' performance. FEC has been widely used as an electrolyte additive as a co-solvent, with a small amount as it is expensive, for metal anodes to improve the stability in Li-ion batteries [59][60][61][62][63]. Moreover, FEC has been shown to participate in the solvation of Li^+ cations but is innocuous to ion transport while passivating the anode surface, resulting in a strong solid electrolyte interface (SEI) with increased LiF production as a fluorine-containing species [35][36]. Our MD simulation results also prove that FEC addition to the PVDF/LiFSI SPEs increases the ionic conductivity (Figure 2a). FEC slightly coordinating the Li^+ (Figure 6) without forming Li^+-solvent clusters (Figures 4c). Thus, it slightly decreases the Li^+ transference number (Figure 2b). Besides, it is dispersed in PVDF/LiFSI SPEs [64], as obtained from our MD simulation results depicted in Figures 3a and 3b.

Jing Zheng et al. demonstrated that an electrolyte composed of LiFSI dissolved in DME, with a controlled amount (12 M LiFSI/DME), suppresses the Li dendritic growth on the anode and stops the polysulfide shuttle reactions on the side of the cathode in the Li-S batteries [62][37]. Besides, as we showed in Figures 2a and 4c, they note that the overall ionic conductivity decreases for a high amount of added DME because of the appearance of big Li^+-solvent aggregates. Also, the Li^+ transference number dramatically decreases with increasing the DME amount. These findings agree with our MD simulation results, depicted in Figures 2a and 2b. In the same context, and line with the results presented in Figure S6b, the DME has a lower viscosity and high flexibility [62][65], qualifying it to construct super-molecular chelating structures, making it capable of solvating the cations [65][66][67][68]. Furthermore, the introduction of DME in its linear form (TEGDME) with the LiFSI, with a regulated amount, is reported to enhance the ionic conductivity in PVDF/LiFSI SPEs and improve interfacial stability by enabling the ultra-long cycle life of metallic Li anodes and preventing the dendrite formation [69].

Wheng et al. investigated the electrochemical intercalation of lithium into a natural graphite anode in quaternary ammonium-based ionic liquid electrolytes. They prove that ES addition into the ionic electrolyte, with a controlled amount, induced electrolyte reduction at a potential of around 1.9 V [70]. The onset potential of the ES solvated Li^+ agrees with those of organic electrolytes containing ES [71][72][73]. Moreover, the decomposition of ES is thought to contribute to the formation of SEI films at the graphite/electrolyte interface [70]. Similarly, ES is known to resist the superoxide radical attack, resulting in an improved

electrochemical performance in Li-O_2 batteries. In particular, high specific capacity, good round-trip efficiency, and cycling stability [74]. Again, the precise control of the SEI formation, using a balanced combination of ES, ethylene carbonate, and vinylene carbonate, makes acetonitrile applicable in lithium-ion batteries without using the superconcentrated formulations necessary to suppress its reductive decomposition [75]. To the best of our knowledge, the effect of ES on the ionic conductivity and Li^+ transference number is not discussed elsewhere. From our MD simulation results, we proved that the addition of ES with little amount than salt slightly affects the ions transport. Whereas, if a significant amount of ES is added to the PVDF/LiFSI SPEs, the ionic conductivity and Li^+ transference number dramatically decrease, as depicted in Figures 2a and 2b.

To sum up, it is clear that the solvents in which the Li^+-FSI^- and Li^+-solvent form small clusters significantly improve the ionic conductivity at room temperature in line with the comparison depicted on figure 7. Moreover, solvents that dissociate the LiFSI ions without trapping or confining the Li^+ ions do not have a significant impact on their transference number. Conversely, solvents that have a strong affinity for Li^+ ions and restrict their movement result in a reduced cations transference number. Similarly, solvents with high diffusion rates and solvents that exhibit a strong affinity for the polymer contribute to an increase in ionic conductivity

5. Conclusions

Large-scale all-atom MD simulations were used to investigate the structural and transport properties of PVDF/LiFSI solid polymer electrolytes in the presence of different solvents. The simulated systems experienced an NPT equilibration followed by 190 ns NVT MD simulations to investigate their structural and dynamic properties. The calculated ionic conductivity values are found in agreement with the available experimental data, validating the accuracy of our simulations. We extensively characterized the solvation structure and arrangement of ions within the PVDF/LiFSI SPEs, revealing valuable insights into the relationship between their structural properties and transport behavior. The calculated ionic conductivity in PVDF/LiFSI SPEs was found to be dependent on the type and amount of adsorbed solvent. Solvents that formed small clusters with Li^+ ions, effectively dissociated the LiFSI ions, and exhibited high diffusion coefficients and strong affinity to the polymer matrix were found to enhance the ionic conductivity. Conversely, excessive interaction strength between Li^+ ions and solvent molecules decreases the cation transference number, thereby reducing the overall ionic conductivity. Based on our assessments, we classify the solvent efficiency for Li^+ transport improvement as follows: DME ($n(DME)/n(Li^+) \leq 1$) > DMF = FEC > NMP > ES = DMSO. This classification reflects the relative influence of each solvent on the enhancement of ionic conductivity within the PVDF/LiFSI SPEs. Future research endeavors will aim to elucidate the underlying factors impacting ionic transport in other PVDF-derived polymers and Li-salts SPEs.

Conflicts of interest

There are no conflicts to declare.

Acknowledgements

We acknowledge the i-site E2S (Energy and Environment Solutions) of the University of Pau and Pays de l'Adour and the municipalities association of Lacq-Orthez for their financial support (No. CONV-2019-0082) through the HUB project RAISE 2024, The Jülich Supercomputing Centre (JSC) for providing a total granted quota of 5056000 core-h on the JUSUF cluster (under the allocations icei-prace-2021-0003), The TGCC for computational facilities of 1500000 core-h (under the project GENCI A0110911484), and the University of Pau and Pays de l'Adour for computational support through the cluster PYRENE.

References

[1] Y.-Y. Sun, Q. Zhang, L. Yan, T.-B. Wang, P.-Y. Hou, A review of interfaces within solid-state electrolytes: fundamentals, issues and advancements, Chemical Engineering Journal (2022) 135179.

[2] C. Sun, J. Liu, Y. Gong, D. P. Wilkinson, J. Zhang, Recent advances in all-solid-state rechargeable lithium batteries, Nano Energy 33 (2017) 363–386.

[3] L. Long, S. Wang, M. Xiao, Y. Meng, Polymer electrolytes for lithium polymer batteries, Journal of Materials Chemistry A 4 (26) (2016) 10038–10069.

[4] J. Lopez, D. G. Mackanic, Y. Cui, Z. Bao, Designing polymers for advanced battery chemistries, Nature Reviews Materials 4 (5) (2019) 312–330.

[5] Q. Zhao, S. Stalin, C.-Z. Zhao, L. A. Archer, Designing solid-state electrolytes for safe, energy-dense batteries, Nature Reviews Materials 5 (3) (2020) 229–252.

[6] L. Bandara, Ak; dissanayake, makl; mellander, b, E. Electrochim Acta 43 (1998) 1447.

[7] L. Fan, Z. Dang, C.-W. Nan, M. Li, Thermal, electrical and mechanical properties of plasticized polymer electrolytes based on peo/p (vdf-hfp) blends, Electrochimica Acta 48 (2) (2002) 205–209.

[8] E. Cha, D. R. Macfarlane, M. Forsyth, C. Lee, Ionic conductivity studies of polymeric electrolytes containing lithium salt with plasticizer, Electrochimica acta 50 (2-3) (2004) 335–338.

[9] H. Pitawala, M. Dissanayake, V. Seneviratne, B.-E. Mellander, I. Albinson, Effect of plasticizers (ec or pc) on the ionic conductivity and thermal properties of the (peo) 9 litf: Al 2 o 3 nanocomposite polymer electrolyte system, Journal of Solid State Electrochemistry 12 (2008) 783–789.

[10] L.-Z. Fan, J. Maier, Composite effects in poly (ethylene oxide)–succinonitrile based all-solid electrolytes, Electrochemistry communications 8 (11) (2006) 1753–1756.

[11] S. K. Patla, A. Roy Choudhury, R. Ray, S. Das, S. Karmakar, Plasticizer ethylene carbonate facilitates new ion coordination site in blend polymer electrolyte: Dielectric relaxation through two-parameter mittag-leffler function, AIP Advances 10 (11) (2020) 115008.

[12] Y. Kumar, S. Hashmi, G. Pandey, Ionic liquid mediated magnesium ion conduction in poly (ethylene oxide) based polymer electrolyte, Electrochimica acta 56 (11) (2011) 3864–3873.

[13] M. Wetjen, M. A. Navarra, S. Panero, S. Passerini, B. Scrosati, J. Hassoun, Composite poly (ethylene oxide) electrolytes plasticized by n-alkyl-n-butylpyrrolidinium bis (trifluoromethanesulfonyl) imide for lithium batteries, ChemSusChem 6 (6) (2013) 1037–1043.

[14] Y.-S. Ye, J. Rick, B.-J. Hwang, Ionic liquid polymer electrolytes, Journal of Materials Chemistry A 1 (8) (2013) 2719–2743.

[15] J.-H. Shin, W. A. Henderson, S. Passerini, Peo-based polymer electrolytes with ionic liquids and their use in lithium metal-polymer electrolyte batteries, Journal of the Electrochemical Society 152 (5) (2005) A978.

[16] K. Karuppasamy, J. Theerthagiri, D. Vikraman, C.-J. Yim, S. Hussain, R. Sharma, T. Maiyalagan, J. Qin, H.-S. Kim, Ionic liquid-based electrolytes for energy storage devices: A brief review on their limits and applications, Polymers 12 (4) (2020) 918.

[17] E. Tocci, C. Rizzuto, F. Macedonio, E. Drioli, Effect of green solvents in the production of pvdf-specific polymorphs, Industrial & Engineering Chemistry Research 59 (12) (2020) 5267–5275.

[18] Y. Liu, B. Xu, W. Zhang, L. Li, Y. Lin, C. Nan, Composition modulation and structure design of inorganic-in-polymer composite solid electrolytes for advanced lithium batteries, Small 16 (15) (2020) 1902813.

[19] X. Judez, M. Piszcz, E. Coya, C. Li, I. Aldalur, U. Oteo, Y. Zhang, W. Zhang, L. M. Rodriguez-Martinez, H. Zhang, et al., Stable cycling of lithium metal electrode in nanocomposite solid polymer electrolytes with lithium bis (fluorosulfonyl) imide, Solid State Ionics 318 (2018) 95–101.

[20] Y. Zheng, Y. Yao, J. Ou, M. Li, D. Luo, H. Dou, Z. Li, K. Amine, A. Yu, Z. Chen, A review of composite solid-state electrolytes for lithium batteries: fundamentals, key materials and advanced structures, Chemical Society Reviews 49 (23) (2020) 8790–8839.

[21] A. S. Best, J. Adebahr, P. Jacobsson, D. MacFarlane, M. Forsyth, Microscopic interactions in nanocomposite electrolytes, Macromolecules 34 (13) (2001) 4549–4555.

[22] S. B. Aziz, T. J. Woo, M. Kadir, H. M. Ahmed, A conceptual review on polymer electrolytes and ion transport models, Journal of Science: Advanced Materials and Devices 3 (1) (2018) 1–17.

[23] M. Zhang, M. Li, Z. Chang, Y. Wang, J. Gao, Y. Zhu, Y. Wu, W. Huang, A sandwich pvdf/hec/pvdf gel polymer electrolyte for lithium ion battery, Electrochimica acta 245 (2017) 752–759.

[24] I. F. Hakem, J. Lal, M. R. Bockstaller, Mixed solvent effect on lithium-coordination to poly (ethylene oxide), Journal of Polymer Science Part B: Polymer Physics 44 (24) (2006) 3642–3650.

[25] J. Theerthagiri, R. A. Senthil, M. H. Ali@ Buraidah, J. Madhavan, A. K. Mohd Arof, Studies of solvent effect on the conductivity of 2-mercaptopyridine-doped solid polymer blend electrolytes and its application in dye-sensitized solar cells, Journal of Applied Polymer Science 132 (35) (2015).

[26] B. Choi, Y. Kim, H. Shin, Ionic conduction in peo–pan blend polymer electrolytes, Electrochimica Acta 45 (8-9) (2000) 1371–1374.

[27] C. Zhou, S. Bag, B. Lv, V. Thangadurai, Understanding the role of solvents on the morphological structure and li-ion conductivity of poly (vinylidene fluoride)-based polymer electrolytes, Journal of The Electrochemical Society 167 (7) (2020) 070552.

[28] C. S. Harris, T. G. Rukavina, Lithium ion conductors and proton conductors: Effects of plasticizers and hydration, Electrochimica acta 40 (13-14) (1995) 2315–2320.

[29] X. Zhang, L. Zhou, Y. Wang, Q. Zhou, Influence of humidity on the complex structure of peo-lithium salt polymer electrolyte, Polymer Science, Series A 60 (2018) 50–56.

[30] G. Foran, D. Mankovsky, N. Verdier, D. Lepage, A. Prébé, D. Aymé-Perrot, M. Dollé, The impact of absorbed solvent on the performance of solid polymer electrolytes for use in solid-state lithium batteries, Iscience 23 (10) (2020) 101597.

[31] B. Commarieu, A. Paolella, S. Collin-Martin, C. Gagnon, A. Vijh, A. Guerfi, K. Zaghib, Solid-to-liquid transition of polycarbonate solid electrolytes in li-metal batteries, Journal of Power Sources 436 (2019) 226852.

[32] Z. Danying, X. Weilin, X. Youyi, Different influences of solvents on pvdf casting solution phase inversion and membrane skin-sublayer structure, ACTA POLYMERICA SINICA (6) (2008) 522–528.

[33] W. Liu, S. W. Lee, D. Lin, F. Shi, S. Wang, A. D. Sendek, Y. Cui, Enhancing ionic conductivity in composite polymer electrolytes with well-aligned ceramic nanowires, Nature energy 2 (5) (2017) 1–7.

[34] A. A. Łatoszyńska, P.-L. Taberna, P. Simon, W. Wieczorek, Proton conducting gel polymer electrolytes for supercapacitor applications, Electrochimica Acta 242 (2017) 31–37.

[35] X. Han, J. Sun, Improved fast-charging performances of phosphorus electrodes using the intrinsically flame-retardant lifsi based electrolyte, Journal of Power Sources 474 (2020) 228664.

[36] T. Hou, G. Yang, N. N. Rajput, J. Self, S.-W. Park, J. Nanda, K. A. Persson, The influence of fec on the solvation structure and reduction reaction of lipf6/ec electrolytes and its implication for solid electrolyte interphase formation, Nano Energy 64 (2019) 103881.

[37] J. Zheng, X. Fan, G. Ji, H. Wang, S. Hou, K. C. DeMella, S. R. Raghavan, J. Wang, K. Xu, C. Wang, Manipulating electrolyte and solid electrolyte interphase to enable safe and efficient li-s batteries, Nano energy 50 (2018) 431–440.

[38] X.-B. Cheng, R. Zhang, C.-Z. Zhao, F. Wei, J.-G. Zhang, Q. Zhang, A review of solid electrolyte interphases on lithium metal anode, Advanced science 3 (3) (2016) 1500213.

[39] H. Yang, J. Li, Z. Sun, R. Fang, D.-W. Wang, K. He, H.-M. Cheng, F. Li, Reliable liquid electrolytes for lithium metal batteries, Energy Storage Materials 30 (2020) 113–129.

[40] E. Peled, S. Menkin, Sei: past, present and future, Journal of The Electrochemical Society 164 (7) (2017) A1703.

[41] A. Wang, S. Kadam, H. Li, S. Shi, Y. Qi, Review on modeling of the anode solid electrolyte interphase (sei) for lithium-ion batteries, npj Computational Materials 4 (1) (2018) 15.

[42] M. Qu, S. Li, J. Chen, Y. Xiao, J. Xiao, Ion transport in the emitfsi/pvdf system at different temperatures: A molecular dynamics simulation, ACS omega 7 (11) (2022) 9333–9342.

[43] S. Kim, M. Lee, C. Park, A. Park, S. Kwon, J. Cho, S. Kim, S. Rho, W. B. Lee, Molecular dynamics study on lithium-ion transport in peo branched nanopores with pyr14tfsi ionic liquid, Battery Energy 1 (2) (2022) 20210013.

[44] F. S. Genier, I. D. Hosein, Effect of coordination behavior in polymer electrolytes for sodium-ion conduction: a molecular dynamics study of poly (ethylene oxide) and poly (tetrahydrofuran), Macromolecules 54 (18) (2021) 8553–8562.

[45] N. Eyvazi, M. Biagooi, S. Nedaaee Oskoee, Molecular dynamics investigation of charging process in polyelectrolyte-based supercapacitors, Scientific Reports 12 (1) (2022) 1098.

[46] X. Shen, H. Hua, H. Li, R. Li, T. Hu, D. Wu, P. Zhang, J. Zhao, Synthesis and molecular dynamic simulation of a novel single ion conducting gel polymer electrolyte for lithium-ion batteries, Polymer 201 (2020) 122568.

[47] H.-S. Liu, K.-Y. Chen, C.-E. Fang, C.-c. Chiu, Comparing the effects of polymer binders on li+ transport near the liquid electrolyte/lifepo4 interfaces: A molecular dynamics simulation study, Electrochimica Acta 375 (2021) 137915.

[48] L. S. Dodda, I. Cabeza de Vaca, J. Tirado-Rives, W. L. Jorgensen, Ligpargen web server: an automatic opls-aa parameter generator for organic ligands, Nucleic acids research 45 (W1) (2017) W331–W336.

[49] S. W. Siu, K. Pluhackova, R. A. Böckmann, Optimization of the opls-aa force field for long hydrocarbons, Journal of Chemical theory and Computation 8 (4) (2012) 1459–1470.

[50] J. N. Canongia Lopes, A. A. Pádua, Cl&p: A generic and systematic force field for ionic liquids modeling, Theoretical Chemistry Accounts 131 (2012) 1–11.

[51] A. P. Thompson, H. M. Aktulga, R. Berger, D. S. Bolintineanu, W. M. Brown, P. S. Crozier, P. J. in't Veld, A. Kohlmeyer, S. G. Moore, T. D. Nguyen, et al., Lammps-a flexible simulation tool for particle-based materials modeling at the atomic, meso, and continuum scales, Computer Physics Communications 271 (2022) 108171.

[52] A. I. Jewett, D. Stelter, J. Lambert, S. M. Saladi, O. M. Roscioni, M. Ricci, L. Autin, M. Maritan, S. M. Bashusqeh, T. Keyes, et al., Moltemplate: A tool for coarse-grained modeling of complex biological matter and soft condensed matter physics, Journal of molecular biology 433 (11) (2021) 166841.

[53] Q. Li, Q. Xue, X. Gao, Q. Zheng, Temperature dependence of the electrical properties of the carbon nanotube/polymer composites, Express Polym Lett 3 (12) (2009) 769–777.

[54] Z. Wang, W. Gao, L. Chen, Y. Mo, X. Huang, Raman and ac impedance spectroscopic studies on roles of polyacrylonitrile in polymer electrolytes, Journal of The Electrochemical Society 149 (5) (2002) E148.

[55] H.-M. Kao, P.-C. Chang, S.-W. Chao, C.-H. Lee, 7li nmr, ionic conductivity and self-diffusion coefficients of lithium ion and solvent of plasticized organic–inorganic hybrid electrolyte based on ppg-peg-ppg diamine and alkoxysilanes, Electrochimica acta 52 (3) (2006) 1015–1027.

[56] N. Voigt, L. van Wüllen, The effect of plastic-crystalline succinonitrile on the electrolyte system peo: Libf4: Insights from solid state nmr, Solid State Ionics 260 (2014) 65–75.

[57] N. Verdier, D. Lepage, R. Zidani, A. Prebe, D. Ayme-Perrot, C. Pellerin, M. Dolle, D. Rochefort, Cross-linked polyacrylonitrile-based elastomer used as gel polymer electrolyte in li-ion battery, ACS Applied Energy Materials 3 (1) (2019) 1099–1110.

[58] P. Yao, B. Zhu, H. Zhai, X. Liao, Y. Zhu, W. Xu, Q. Cheng, C. Jayyosi, Z. Li, J. Zhu, et al., Pvdf/palygorskite nanowire composite electrolyte for 4 v rechargeable lithium batteries with high energy density, Nano letters 18 (10) (2018) 6113–6120.

[59] R. McMillan, H. Slegr, Z. Shu, W. Wang, Fluoroethylene carbonate electrolyte and its use in lithium ion batteries with graphite anodes, Journal of Power Sources 81 (1999) 20–26.

[60] K. Schroder, J. Alvarado, T. A. Yersak, J. Li, N. Dudney, L. J. Webb, Y. S. Meng, K. J. Stevenson, The effect of fluoroethylene carbonate as an additive on the solid electrolyte interphase on silicon lithium-ion electrodes, Chemistry of Materials 27 (16) (2015) 5531–5542.

[61] Y. Jin, N.-J. H. Kneusels, L. E. Marbella, E. Castillo-Martínez, P. C. Magusin, R. S. Weatherup, E. Jónsson, T. Liu, S. Paul, C. P. Grey, Understanding fluoroethylene carbonate and vinylene carbonate based electrolytes for si anodes in lithium ion batteries with nmr spectroscopy, Journal of the American Chemical Society 140 (31) (2018) 9854–9867.

[62] X.-Q. Zhang, X.-B. Cheng, X. Chen, C. Yan, Q. Zhang, Fluoroethylene carbonate additives to render uniform li deposits in lithium metal batteries, Advanced Functional Materials 27 (10) (2017) 1605989.

[63] J. Wan, Y. Hao, Y. Shi, Y.-X. Song, H.-J. Yan, J. Zheng, R. Wen, L.-J. Wan, Ultra-thin solid electrolyte interphase evolution and wrinkling processes in molybdenum disulfide-based lithium-ion batteries, Nature communications 10 (1) (2019) 3265.

[64] Y. Liu, Y. Xu, Porous membrane host-derived in-situ polymer electrolytes with double-stabilized electrode interface enable long cycling lithium metal batteries, Chemical Engineering Journal 433 (2022) 134471.

[65] Z. Jiang, Z. Zeng, X. Liang, L. Yang, W. Hu, C. Zhang, Z. Han, J. Feng, J. Xie, Fluorobenzene, a low-density, economical, and bifunctional hydrocarbon cosolvent for practical lithium metal batteries, Advanced Functional Materials 31 (1) (2021) 2005991.

[66] K. Xu, Nonaqueous liquid electrolytes for lithium-based rechargeable batteries, Chemical reviews 104 (10) (2004) 4303–4418.

[67] D.-R. Chang, S.-H. Lee, S.-W. Kim, H.-T. Kim, Binary electrolyte based on tetra (ethylene glycol) dimethyl ether and 1, 3-dioxolane for lithium–sulfur battery, Journal of Power Sources 112 (2) (2002) 452–460.

[68] O. Borodin, L. Suo, M. Gobet, X. Ren, F. Wang, A. Faraone, J. Peng, M. Olguin, M. Schroeder, M. S. Ding, et al., Liquid structure with nanoheterogeneity promotes cationic transport in concentrated electrolytes, ACS nano 11 (10) (2017) 10462–10471.

[69] Q. Liu, Y. Liu, X. Jiao, Z. Song, M. Sadd, X. Xu, A. Matic, S. Xiong, J. Song, Enhanced ionic conductivity and interface stability of hybrid solid-state polymer electrolyte for rechargeable lithium metal batteries, Energy Storage Materials 23 (2019) 105–111.

[70] H. Zheng, K. Jiang, T. Abe, Z. Ogumi, Electrochemical intercalation of lithium into a natural graphite anode in quaternary ammonium-based ionic liquid electrolytes, Carbon 44 (2) (2006) 203–210.

[71] D. Aurbach, K. Gamolsky, B. Markovsky, Y. Gofer, M. Schmidt, U. Heider, On the use of vinylene carbonate (vc) as an additive to electrolyte solutions for li-ion batteries, Electrochimica acta 47 (9) (2002) 1423–1439.

[72] G. H. Wrodnigg, J. O. Besenhard, M. Winter, Ethylene sulfite as electrolyte additive for lithium-ion cells with graphitic anodes, Journal of The Electrochemical Society 146 (2) (1999) 470.

[73] M. Fujimoto, Y. Shoji, Y. Kida, R. Ohshita, T. Nohma, K. Nishio, Influence of solvent species on the charge–discharge characteristics of a natural graphite electrode, Journal of power sources 72 (2) (1998) 226–230.

[74] C. Wu, C.-B. Liao, L. Li, J. Yang, Ethylene sulfite based electrolyte for non-aqueous lithium oxygen batteries, Chinese Chemical Letters 27 (9) (2016) 1485–1489.

[75] N. Matsuoka, H. Kamine, Y. Natsume, A. Yoshino, Moderately concentrated acetonitrile-containing electrolytes with high ionic conductivity for durability-oriented lithium-ion batteries, ChemElectroChem 8 (16) (2021) 3095–3104.